Report PME-FM-84-1

INJECTION OF DRAG REDUCING ADDITIVES INTO TURBULENT WATER FLOWS

Results from Factorial Design

David T. Walker and William G. Tiederman
School of Mechanical Engineering
Purdue University
West Lafayette, Indiana 47907

April 1984

Technical Report for Period 23 March 1983 - 23 February 1984

Prepared for

OFFICE OF NAVAL RESEARCH
800 No. Quincey St.
Arlington, VA 22217

SECURITY CLASSIFICATION OF THIS PAGE (When Data Entered)

REPORT DOCUMENTATION PAGE

READ INSTRUCTIONS BEFORE COMPLETING FORM

1. REPORT NUMBER: PME-FM-84-1	2. GOVT ACCESSION NO.
3. RECIPIENT'S CATALOG NUMBER	
4. TITLE (and Subtitle): INJECTION OF DRAG REDUCING ADDITIVES INTO TURBULENT WATER FLOWS: Results from Factorial Design	5. TYPE OF REPORT & PERIOD COVERED: Annual Report March 1, 1983 through February 29, 1984
	6. PERFORMING ORG. REPORT NUMBER
7. AUTHOR(s): David T. Walker and William G. Tiederman	8. CONTRACT OR GRANT NUMBER(s): N0014-83K-0183
9. PERFORMING ORGANIZATION NAME AND ADDRESS: School of Mechanical Engineering, Purdue University, West Lafayette, Indiana 47907	10. PROGRAM ELEMENT, PROJECT, TASK AREA & WORK UNIT NUMBERS: 61153N 23 RR02301 NR062-754
11. CONTROLLING OFFICE NAME AND ADDRESS: Office of Naval Research, 800 N. Quincey St., Arlington, VA 22217	12. REPORT DATE: April 1984
	13. NUMBER OF PAGES: 47
14. MONITORING AGENCY NAME & ADDRESS (if different from Controlling Office)	15. SECURITY CLASS. (of this report)
	15a. DECLASSIFICATION/DOWNGRADING SCHEDULE

16. DISTRIBUTION STATEMENT (of this Report)

APPROVED FOR PUBLIC RELEASE: DISTRIBUTION UNLIMITED

17. DISTRIBUTION STATEMENT (of the abstract entered in Block 20, if different from Report)

18. SUPPLEMENTARY NOTES

19. KEY WORDS (Continue on reverse side if necessary and identify by block number)

Drag reduction; Turbulent wall flows

20. ABSTRACT (Continue on reverse side if necessary and identify by block number)

The basic objective of this experimental study is to optimize the process of injecting drag-reducing additives into a water flow. The initial phase consisted of a factorial design where the concentration and flowrate of the injected additive as well as the angle and width of the injection slot were varied independently. The experiments were conducted in a rectangular cross section channel that has an aspect ratio of ten to one. Slots were located in both of the larger walls at a streamwise location where the channel flow of -> cont

DD FORM 1 JAN 73 1473 EDITION OF 1 NOV 65 IS OBSOLETE
S/N 0102-014-6601

SECURITY CLASSIFICATION OF THIS PAGE (When Data Entered)

water was fully developed. Drag reduction was deduced from wall pressure measurements and wall-layer concentration of the additive was deduced from colorimeter measurements. Additive concentration varied from 100 to 400 ppm. Injection flowrates ranged from 200 to 400 ml/min. The slot angle was either 15 or 25 degrees while the slot width was either 1.27 mm or 2.54 mm. The quantity which was optimized (the merit function) was the integral of the drag reduction with respect to streamwise distance beginning at the initial location of positive drag reduction and ending at the location where the additive was uniformly mixed with the water.

Statistical analysis of the results showed that for the range of variable studied, the merit function depends primarily upon the linear terms for additive concentration and injection flow rate. The product of additive concentration and injection flowrate as well as the product of slot angle and slot width were significant but less important factors in fitting the experimental response. The analysis indicated that the largest increase in the merit function would be achieved by increasing the injection flow rate and additive concentration.

The results showed that additive concentrations less than 1 ppm yield drag reduction on the order of 20%. These results were achieved well downstream of the injector where it is hypothesized that the additive molecules were in an excellent conformation for reducing drag.

TABLE OF CONTENTS

INTRODUCTION

It is well known that the presence of dilute solutions of high molecular weight polymers in the near-wall region of bound turbulent shear flows can reduce the wall shear stress. As shown by recent studies at Purdue (1,2) and by McComb and Rabie (3), the additives have a direct effect upon the flow structures in the buffer layer, $10 < y^+ < 100$. The purpose of this study was to develop experimentally, optimum methods for the injection of polymer additives into a turbulent water flow. The specific objectives were to maximize the reduction of viscous drag downstream of the injection slot and to build a data base for the diffusion characteristics of the injected additives.

These experiments were conducted in a 2.5 cm by 25 cm rectangular cross section channel. The additive solutions were injected into the fully developed turbulent water flow through slots in the 25 cm walls. Drag reduction was deduced from pressure drop measurements made upstream and downstream of the injection slots with and without additive injection. Measurements of the additive concentration in the near-wall region were obtained by withdrawing samples of fluid from this region during injection.

The optimization program was begun by testing all combinations of two levels of each independent variable governing the injection and diffusion processes. These were the angle and width of the injection slot and the concentration and flowrate of

the additive solution. The results of these experiments were analyzed statistically using the techniques of response surface methodology to determine the most efficient way to approach the optimum combination of these four variables.

There have been several other experimental programs where the injection process has been studied. For example Maus and Wilhelm (4) examined the effect of additive injection on drag in a pipe with five circumferential slots located six inches apart. While they varied injection flowrates and determined an optimum injection concentration for each injection pattern, they did not vary the design of the slots.

Walters and Wells (5) discussed the desirability of reducing an anomalous drag increase detected in their studies of injection through a porous wall. They varied injection flowrate and injection concentration for different lengths of porous wall injection. However, similar to Maus & Wilhem there was not an independent variation in the porosity of the injector.

More recently an anomalous drag increase near the injector was reported and discussed by Fruman and Dalivel (6,7). In addition to decreases in mixing as concentration increases they reported swelling of the injected material as it leaves the slot.

The studies of Wu and Tulin (8) and Wu (9) included systematic variations in injection flowrate, concentration of injected fluid and injector design. However, in these two studies the total drag on a flat plate of fixed streamwise length

was measured. In this study the static wall pressure downstream of the injection was measured. From this streamwise pressure distribution one directly measures any adverse drag increase and determines the streamwise length over which the injection is effective. The latter is crucial for determining the need and location for a second slot.

The present experiments were conducted in the fully developed region of a turbulent channel flow. Consequently they differed significantly from the studies at Colorado State (10, 11) where the drag-reducing additive was injected into the strong favorable pressure gradient in the entrance region of a pipe.

There have also been several studies where the diffusion of a drag-reducing additive from the wall region has been studied (12, 13, 14, 15). While these studies have provided valuable insights, including the conclusion that large injection concentrations can yield unnecessarily large concentrations in the wall region (14), they have not yet lead to methods for achieving an optimum design for the injection process.

EXPERIMENTAL APPARATUS AND PROCEDURES

Apparatus

The experiments were performed in the recirculating flow loop shown in Figure 1. The flow loop incorporates a combination of a perforated plate, a screen-sponge-screen section, smooth contractions and flow straighteners to ensure a smooth flow at the inlet of the two dimensional channel. The flowrate in the channel is monitored using an orifice meter connected to an inverted U-tube manometer.

The test section of the channel has a rectangular cross-section, with internal dimensions of 2.5 cm by 25 cm resulting in an aspect ratio of ten to one. The injection slots are located more than one hundred channel widths downstream of the inlet and approximately eighty channel widths upstream of the exit. Consequently, the flow at the injection point is typical of fully developed, two-dimensional channel flow.

The additive solutions were injected through removable slots located in both of the 25 cm walls of the test section. Pressure drop measurements were obtained from thirteen pressure taps located along the centerline of one of the 25 cm walls. The relative locations of the slots and pressure taps are shown in Figure 2. The injection slots, also shown in Figure 2, are in brass inserts that span the channel in the 25 cm walls. The slots have a length, in the spanwise direction, of 22.44 cm and their geometry is defined by the slot width (d) measured in the

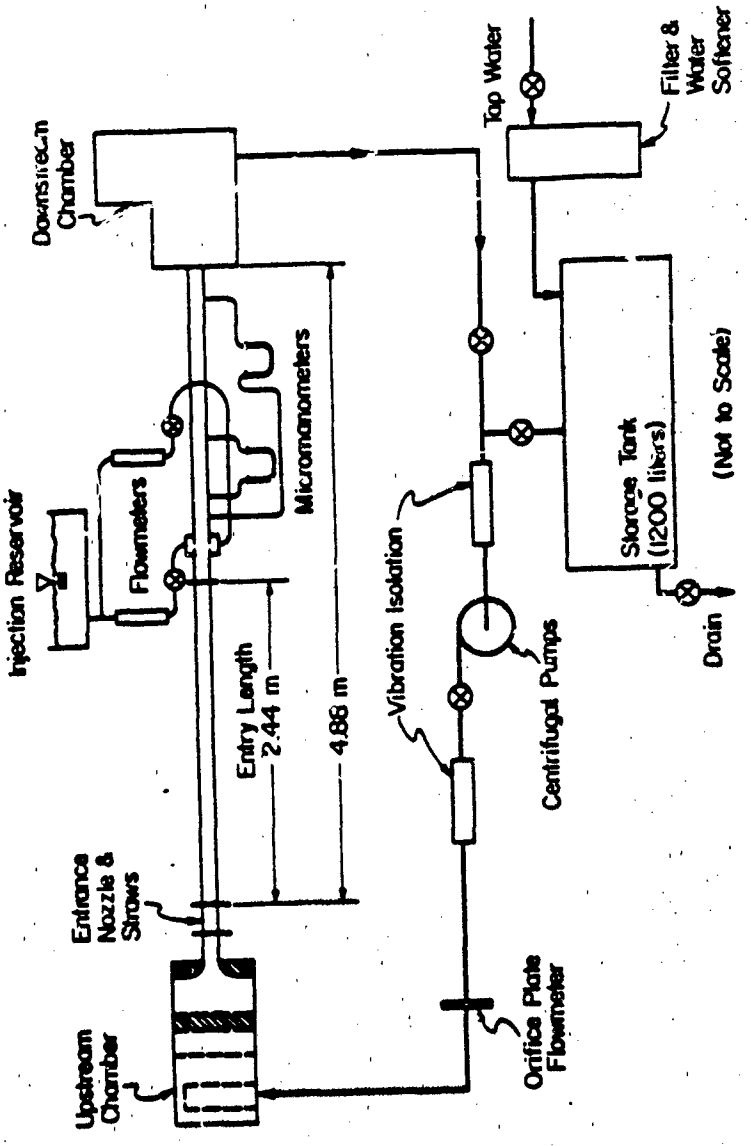

Figure 1. Schematic of flow loop.

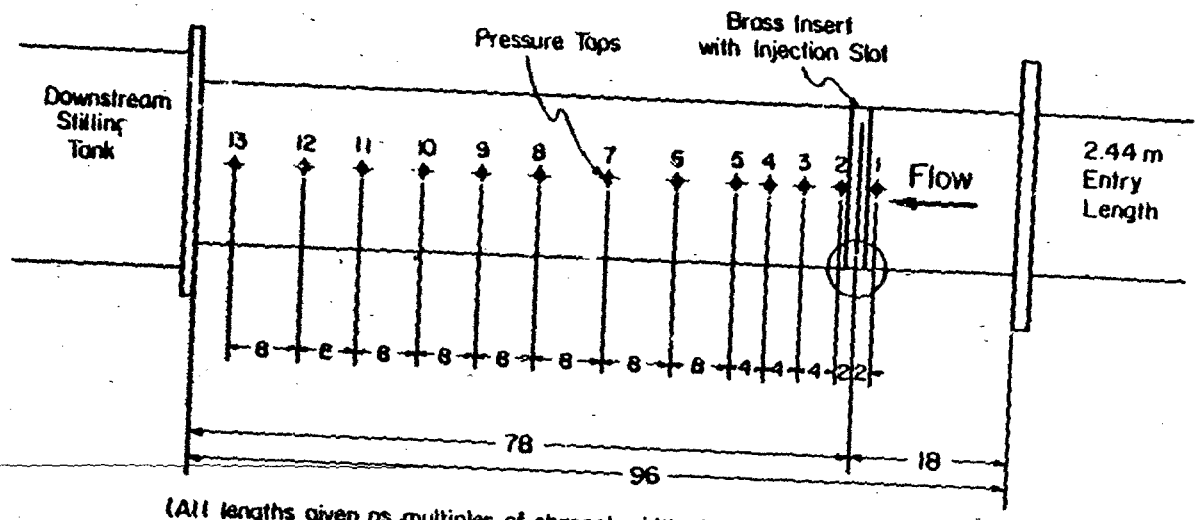

(All lengths given as multiples of channel width. W=2.5 cm)

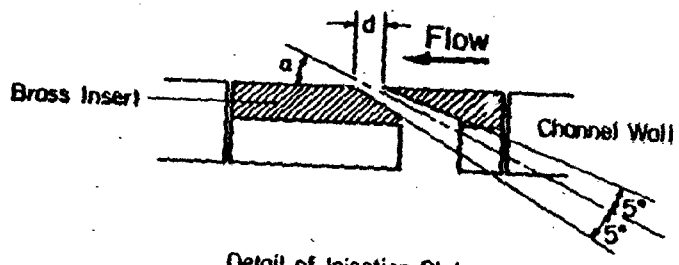

Detail of Injection Slot

Figure 2. Schematic of test section showing injection slot and pressure tap locations, and cross sectional view of injection slot.

streamwise direction and the angle of inclination of the outlet to the flow direction in the channel (α). The slots are machined with an included angle of five degrees and the angle of inclination is measured to the bisector of this included angle. For this study, slot widths of 2.54 mm and 1.27 mm were used along with slot angles of 15 and 25 degrees.

Pressure drop measurements were made with two Gilmont micrometer manometers. The manometer fluid used was carbon tetrachloride resulting in a measurement sensitivity of 0.015 mm of water.

The additives were dilute solutions of SEPARAN AP-273, a polyacrylimide manufactured by Dow Chemical Corp. Solutions with concentrations of 100 ppm and 400 ppm by weight were gravity fed to the injector slots from an overhead reservoir. The injection flowrate was regulated using a metering valve and a Gilmont rotameter flow meter for each slot. The flow meters were calibrated for each concentration of the additive.

Concentration measurements were made using a Bausch and Lomb Spectronic 20 Spectrophotometer to measure the dye concentration in samples drawn from the channel while injecting dyed additive solutions. Using an initial dye concentration of 2 g/l of Flourescein disodium salt resulted in an uncertainty at 20 to 1 odds of four percent for measured dye concentrations greater than one percent of the initial dye concentration. The uncertainty increased to twenty percent for measured dye concentrations

between one-tenth of one percent and one percent of the initial dye concentration.

Procedures

Prior to an experiment, filtered softened tap water for the flow loop was deaerated by heating to approximately 50°C in a separate holding tank. This water was then cooled to room temperature before being introduced into the flow loop.

Preparation of the additive solutions consisted of two steps. The solutions were initially mixed to a concentration of 2670 ppm and allowed to hydrate for twelve to twenty-four hours. These solutions were then diluted to their final concentration, either 100 ppm or 400 ppm, and allowed to hydrate for another twelve to twenty-four hours before being used. Filtered tap water was used in the preparation of all solutions.

Prior to each experiment the drag reducing capability of each batch of additive was established using a horizontal 1.405 cm I.D. tube. The additive was gravity fed to the tube with the flowrate controlled by a valve at the tube outlet. The flowrate through the tube was measured along with the pressure drop across two taps, one located more than 30 tube diameters downstream of the inlet and the other more than 15 diameters upstream of the outlet. The distance between these taps is two meters. The viscosities of the additives were measured with a Wells-Brookfield LVT-SCP 1.°65° cone and plate micro viscometer at shear rates of 115 and 230 sec^{-1}.

Drag reduction was calculated from pressure drop measurements taken with and without additive injection. The sequence of steps for the pressure drop measurements were as follows. First with the pumps turned off and water in the channel, a zero reading for the manometer was taken. The loop was then started and the pressure drop across a pair of taps was measured. Once the "without-injection" pressure drop was measured, the injectors were turned on and the pressure drop with additive injection was measured. The injection was then terminated and the "without-injection" pressure drop was remeasured. Finally the flow was stopped and the zero was remeasured. If the second "without-injection" pressure drop and zero measurements were in agreement with the first ones, the manometer was connected to the next pair of pressure taps in preparation for the next sequence of measurements. In the event that the repeated readings did not reproduce the initial measurements, the sequence was repeated for that pair of taps.

Since these experiments were conducted in a recirculating flow loop, there is the potential for an accumulation of additive in the water, resulting in drag reduction without injection. Therefore, the condition of the water in the flow loop during an experiment was monitored by periodically measuring the pressure drop across a specified pair of pressure taps. A decrease in the measured pressure drop across these two taps would indicate that drag reduction due to additive accumulation was occurring. It should be noted that this problem was not encountered during

these experiments.

The additive solution used for wall concentration measurements was dyed with 2.0 grams per liter Flourescein disodium salt. Samples were drawn from wall taps during the injection of the dyed solution and the dye corcentration of the samples was measured. The sampling rate for all concentration measurements was 20 ml/min. The rationale for this sampling rate is discussed in Appendix A.

RESULTS

In all of the experiments, the water temperature in the channel was maintained at 24°C and the channel flowrate was 240 liters per minute yielding a Reynolds number of 17,800 based on channel width. All combinations of two levels for each of the independent variables were tested. The independent variables were slot angle, slot width, injection flowrate and injection concentration. The levels of these variables and the combinations tested are summarized in Table 1.

Table 1. Experimental conditions

SLOT ANGLE (degrees)	SLOT WIDTH (mm)	INJECTION FLOWRATE (ml/min)	INJECTION CONCENTRATION (ppm)
25	2.54	400	400
"	"	"	100
"	"	200	400
"	"	"	100
"	1.27	400	400
"	"	"	100
"	"	200	400
"	"	"	100
15	2.54	400	400
"	"	"	100
"	"	200	400
"	"	"	100
"	1.27	400	400
"	"	"	100
"	"	200	400
"	"	"	100

As stated previously, drag reduction was deduced from pressure drop measurements made in the channel. These measurements provide an indirect measure of the wall shear stress in the channel and therefore a measure of the change in magnitude of the

viscous drag when the additive solution is present. For a fully developed channel flow, the average wall shear stress over a given length of the channel is proportional to the pressure drop over that length. The fully developed assumption is not applicable in the vicinity of the injection slots when fluid is being injected, nontheless the pressure drops still yield the best estimate of the viscous drag. Hence, in this study drag reduction is calculated from

$$DR = \frac{\Delta P - \Delta P)_i}{\Delta P}$$

where $\Delta P)_i$ is the pressure drop when an additive is being injected and ΔP is the pressure drop for the fully developed channel flow without injection.

Figures 3 through 6 show the variation of drag reduction as a function of dimensionless distance (x^+) downstream of the injection slot. The distance (x) is normalized with the shear velocity of the channel flow without injection and the kinematic viscosity of the channel water. The level of drag reduction measured between two taps is indicated by a horizontal line, spanning the distance between the taps, with a vertical bar at each end. The vertical line with horizontal bars through the point indicates the uncertainty for a 95% confidence interval. The points are plotted at the streamwise location midway between the two taps. Each figure compares the performance of the various slot geometries for a given injection flowrate and concentration. The four figures cover the range of flowrates and

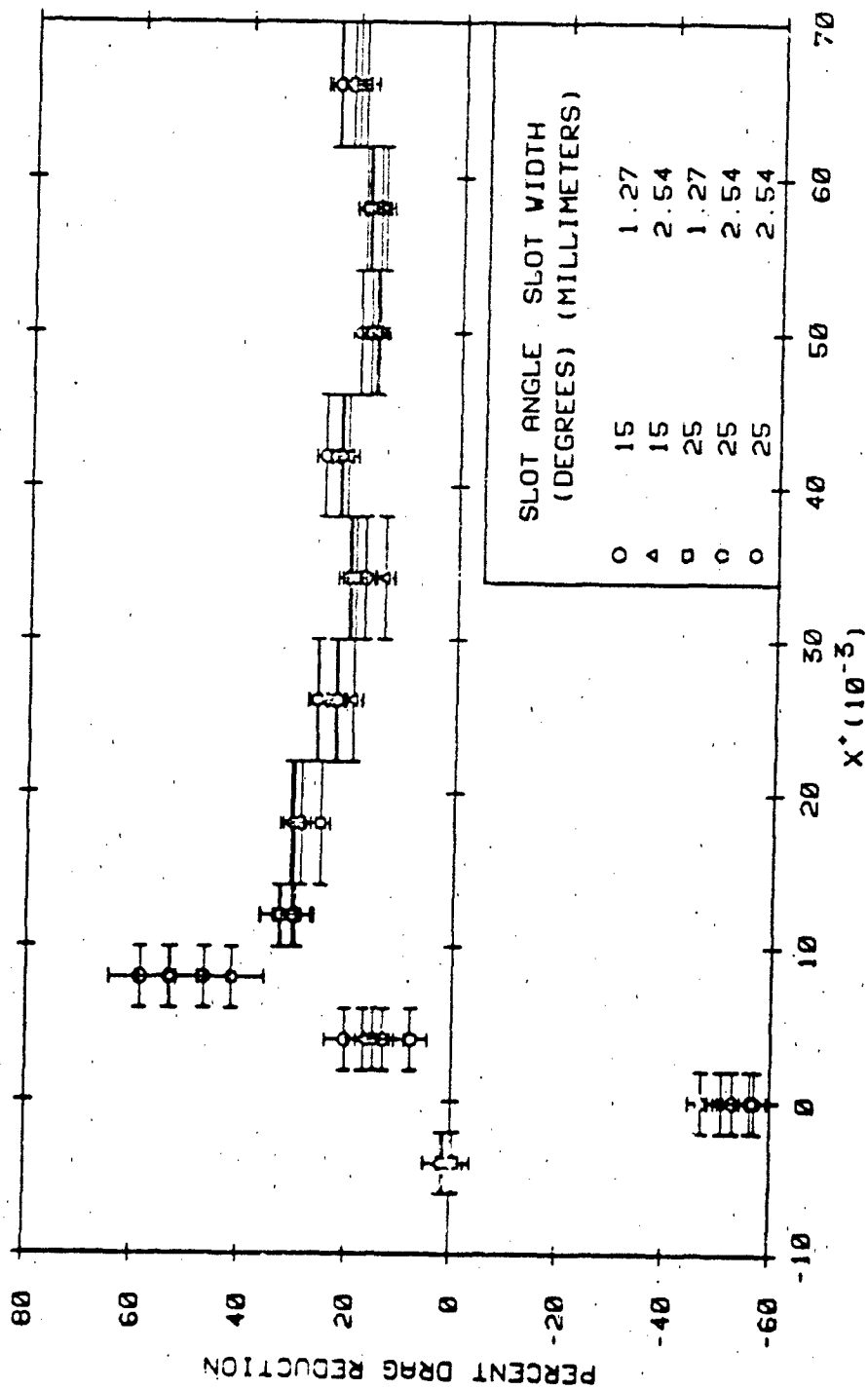

Figure 3. Comparison of various slot geometries for an injection flowrate of 400 ml/min and an injection concentration equal to 400 ppm.

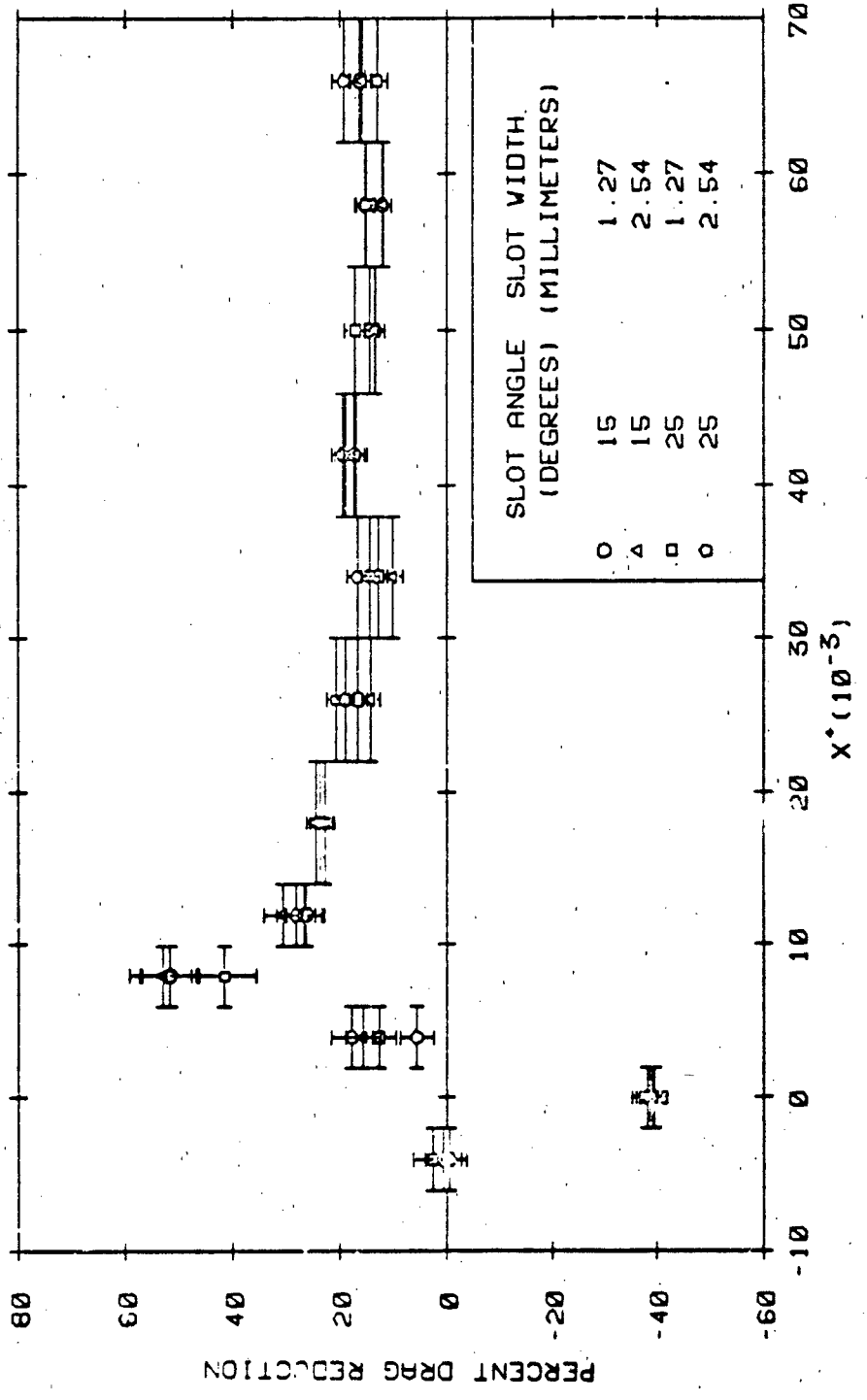

Figure 4. Comparison of various slot geometries for an injection flowrate of 200 ml/min and an injection concentration equal to 400 ppm.

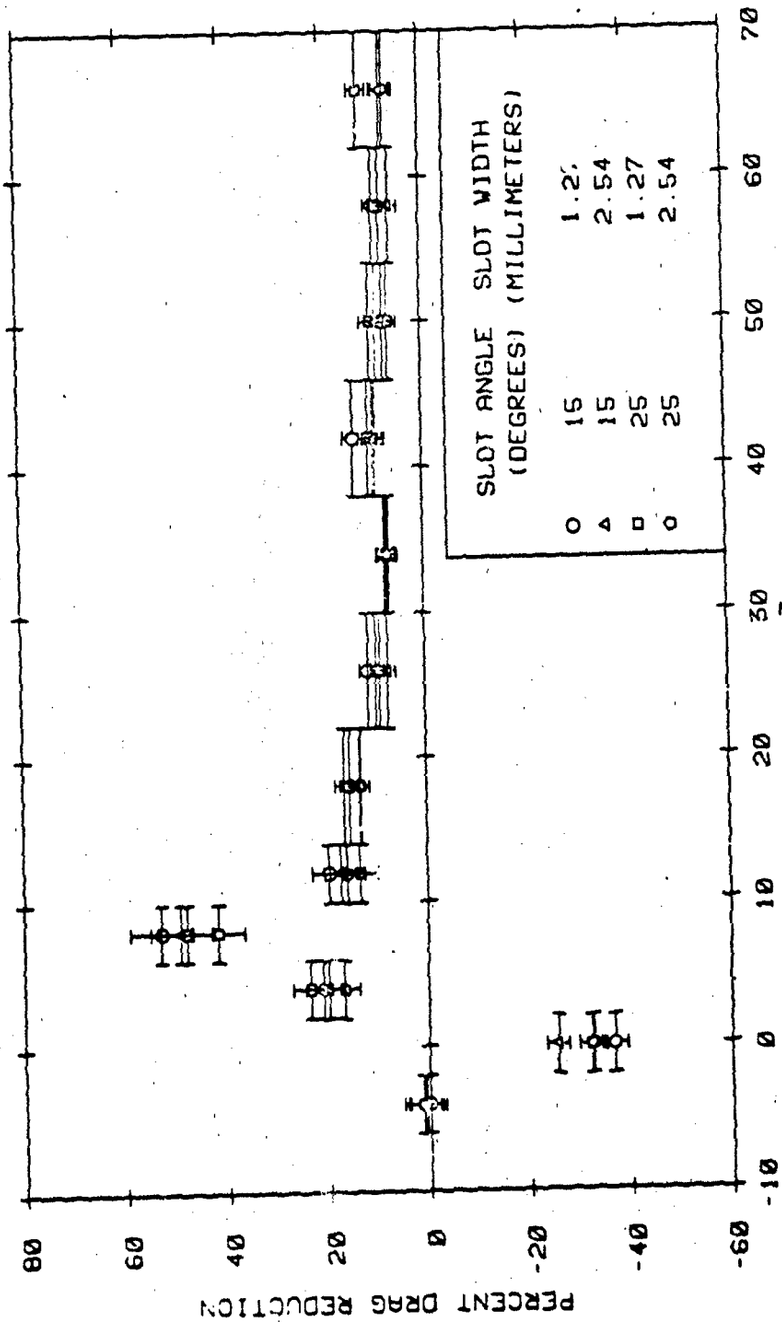

Figure 5. Comparison of various slot geometries for an injection flowrate of 400 ml/min and an injection concentration equal to 100 ppm.

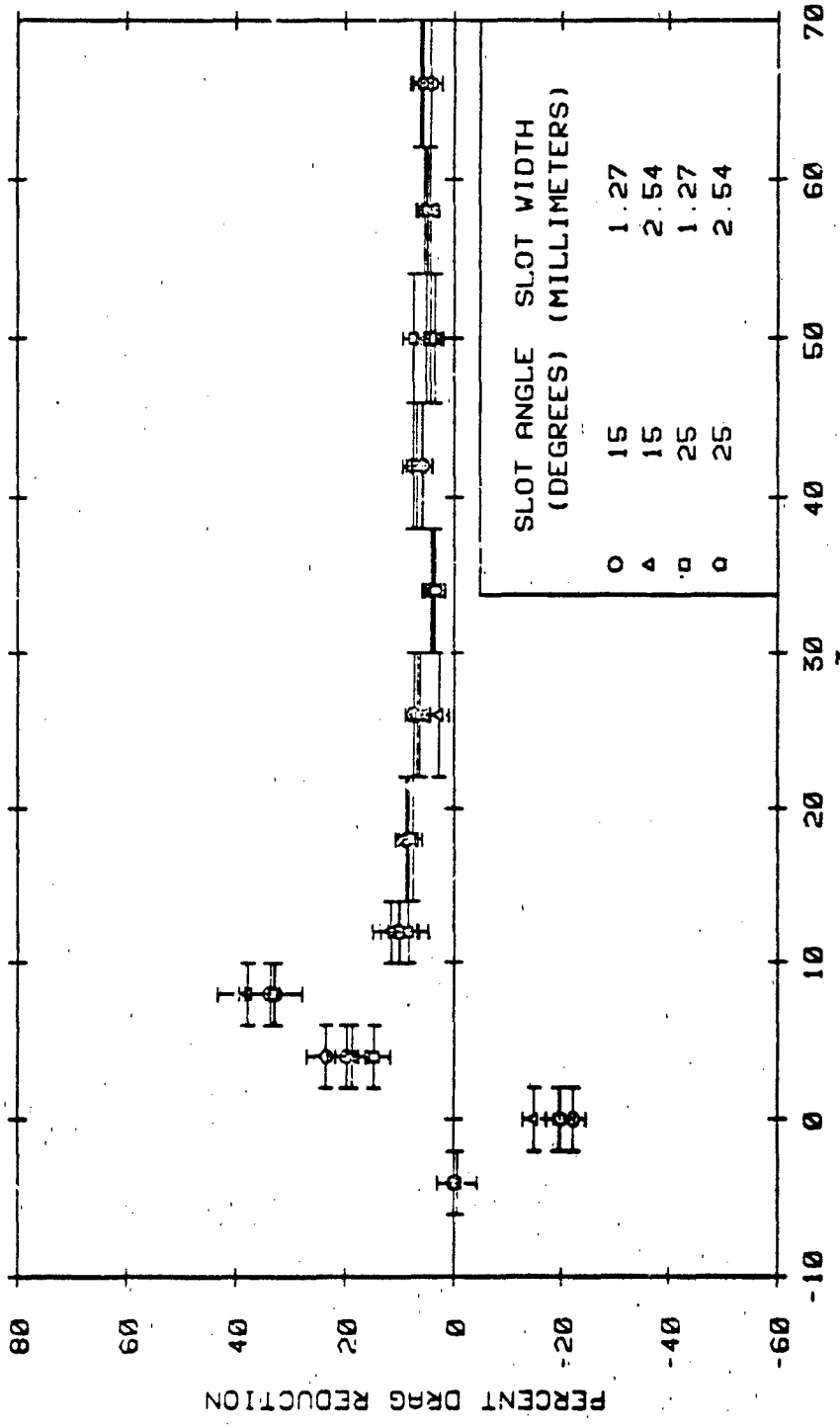

Figure 6. Comparison of various slot geometries for an injection flowrate of 200 ml/min and an injection concentration equal to 100 ppm.

concentrations tested in this study.

The dominant characteristics of Figures 3 through 6 is the small influence of the slot width and slot angle upon the resulting drag reduction. The lack of geometric dependence shown in Figures 3-6 could be the result of a constraint introduced in the choice of the initial levels of the four independent variables. It was known from previous experiments that when the injection momentum flux through a 0.125 mm slot that was normal to the flow direction exceeded approximately 1/30 the streamwise momentum flux through the viscous sublayer that the injected fluid would not turn and flow downstream along the wall but would jet out into the main flow. In the interest of keeping the injected solutions in the near-wall region for as long as possible, the combinations of flowrates and slot geometries for these initial experiments were chosen so that the normal momentum fluxes were of the order of 1/30 the sublayer streamwise momentum flux. Dimensionless normal momentum fluxes $\langle M^+ \rangle$ for each flowrate - slot geometry combination are tabulated in Table 2. Since slot width is, by definition, measured in the streamwise direction, normal momentum flux is dependent on slot width only and is independent of slot angle. The values of momentum flux are normalized with 1/30 the sublayer momentum flux.

Table 2. Dimensionless normal momentum flux of injected solutions.

INJECTION FLOWRATE (ml/min)	SLOT WIDTH (mm)	M^+
400	2.54	1.80
400	1.27	3.60
200	2.54	0.45
200	1.27	0.90

This constraint on the injection normal momentum flux did yield injections that initially remained in the near-wall region. This was confirmed by side view flow visualization of dyed injections. For all of the geometries studied, the additive left the injection slot as a thin sheet flowing over the downstream edge of the injector. There was no evidence of a jet emanating from any of the injectors tested. Since the combinations of injection flowrates and slot geometries that were tested did not cause the additive solutions to jet away from the wall, the only influence of slot geometry was to modify the initial mixing of the injected additive with the water flow.

Figures 7 through 10 show comparisons of the performance of a given slot when tested at various injection flowrates and concentrations. The four figures cover the range of slot geometries tested. It can be seen from these figures that, in general, the levels of drag reduction measured increase with mass flow rate of polymer. It is also evident that drag reduction does not increase linearly with the product of injection flow rate and concentration.

It should be noted that Figure 10 shows two experiments

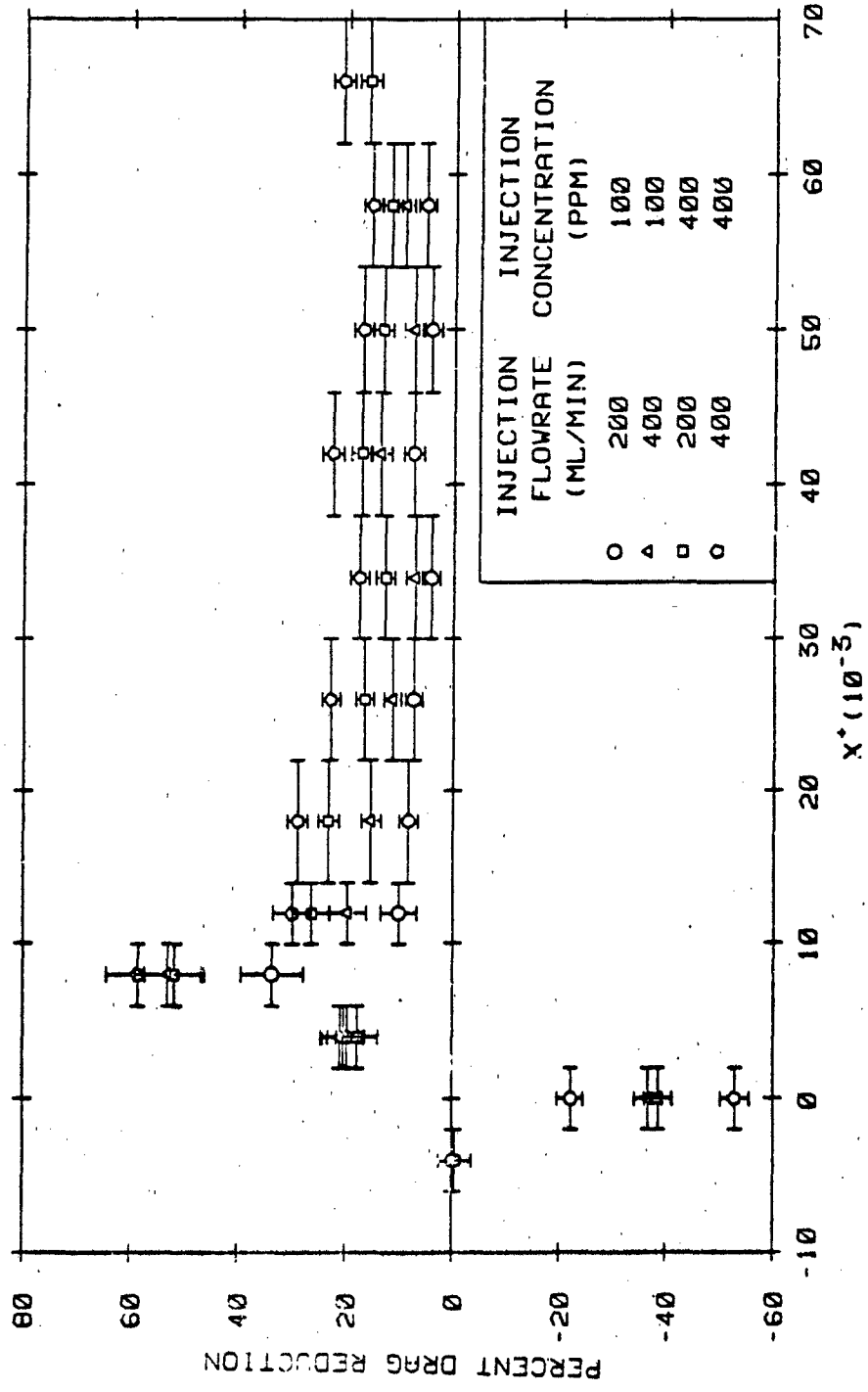

Figure 7. Comparison of various injection flowrates and concentrations for a slot angle of 15 degrees and a slot width equal to 1.27 mm.

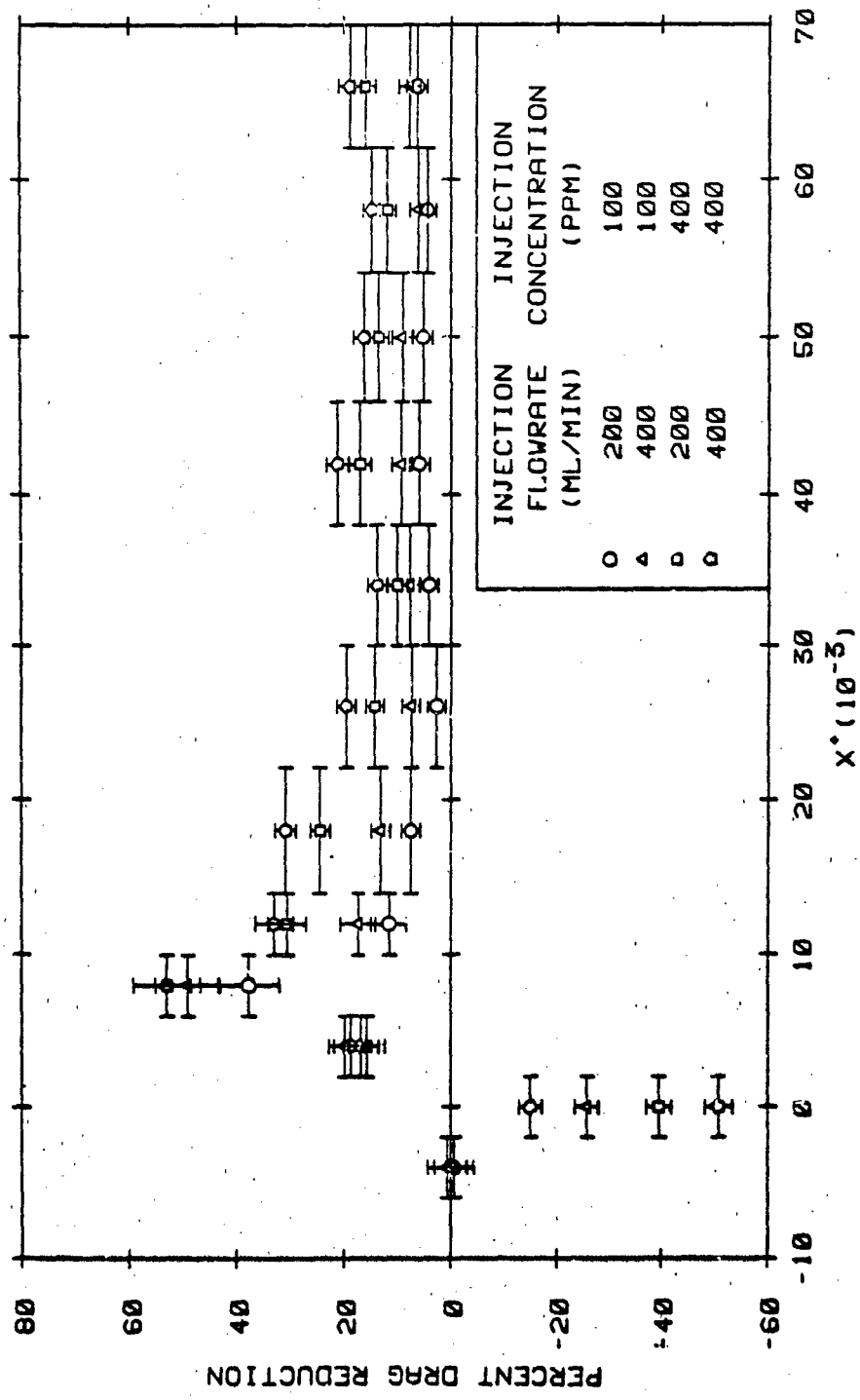

Figure 8. Comparison of various injection flowrates and concentrations for a slot angle of 15 degrees and a slot width equal to 2.54 mm.

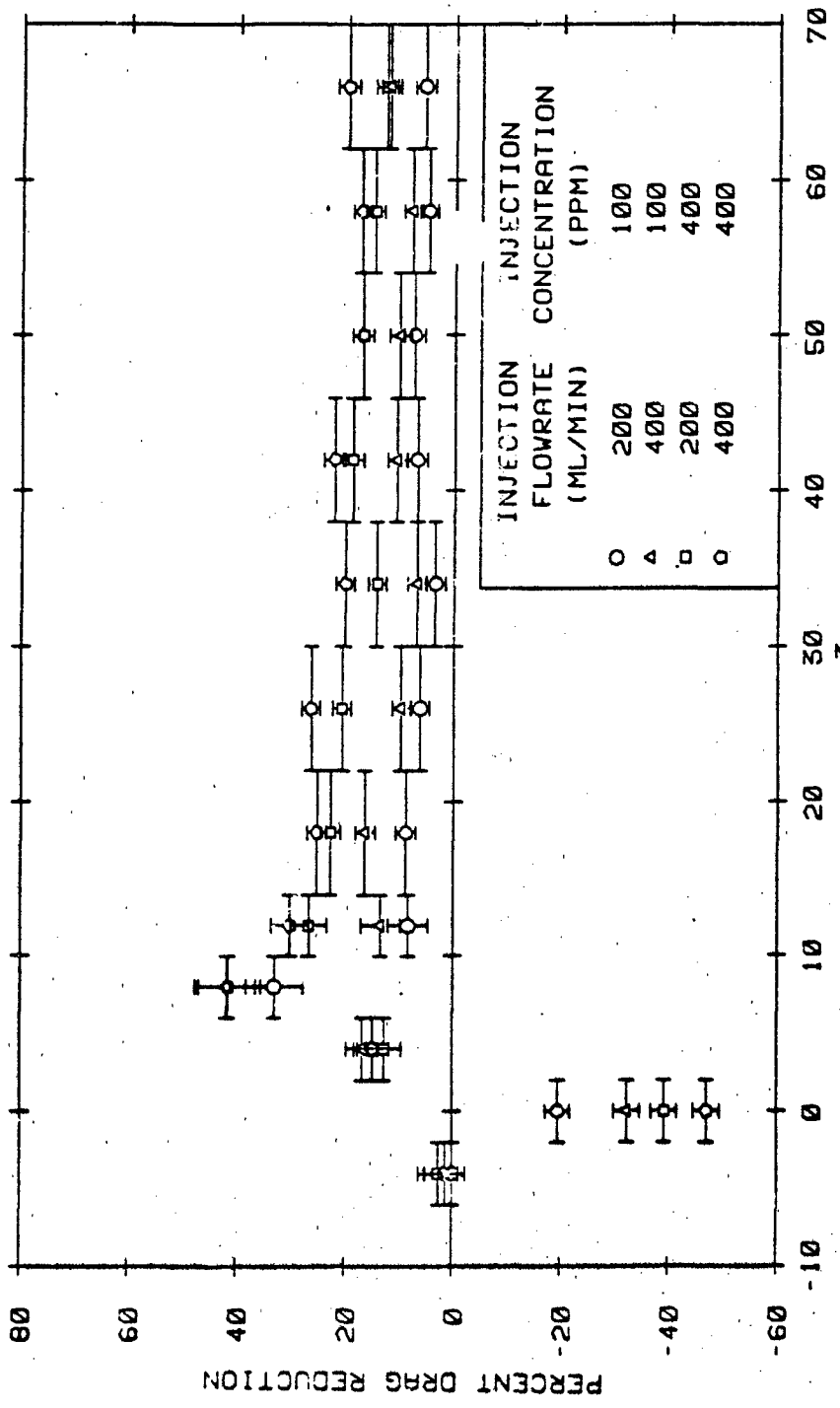

Figure 9. Comparison of various injection flowrates and concentrations for a slot angle of 25 degrees and a slot width equal to 1.27 mm.

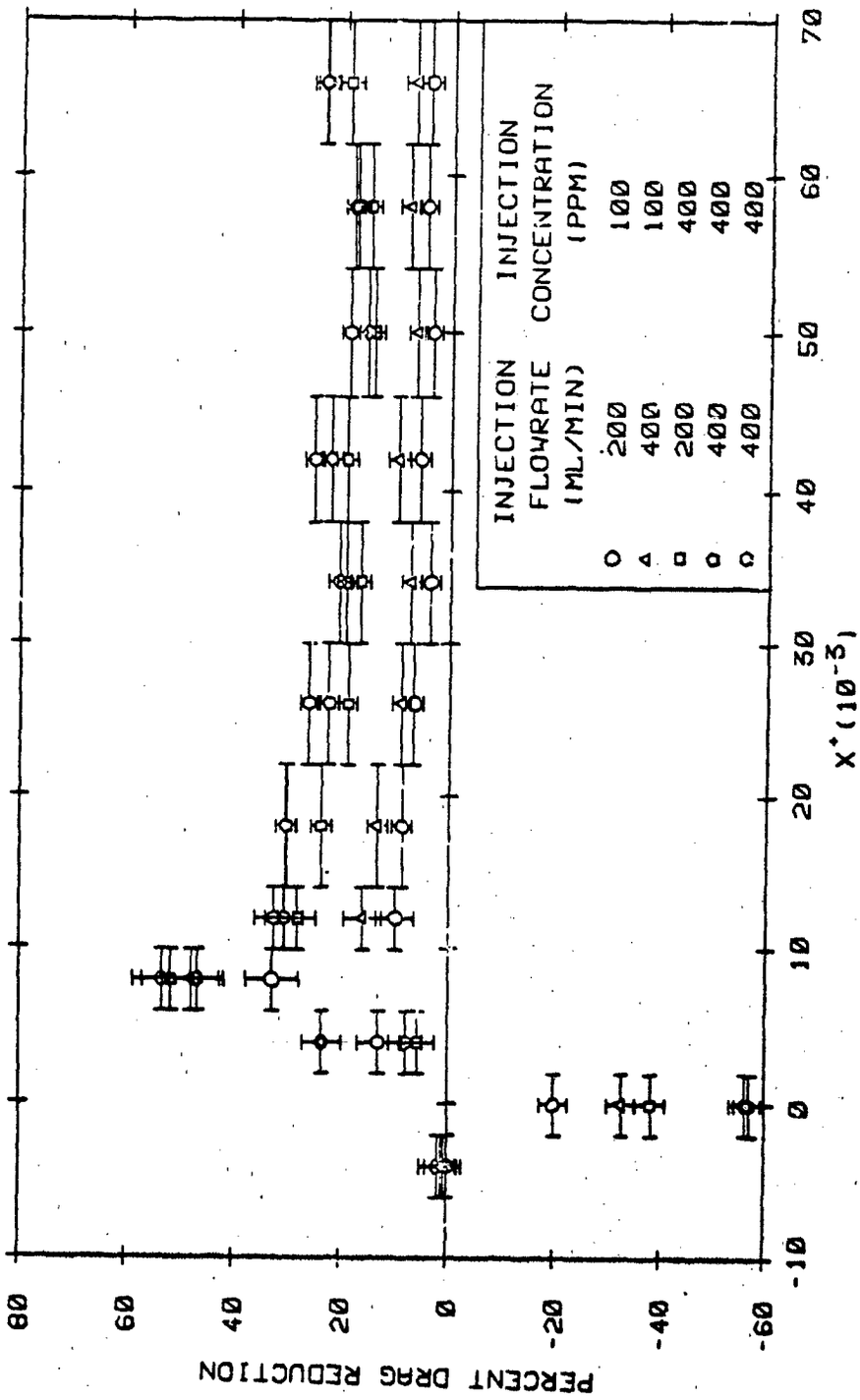

Figure 10. Comparison of various injection flowrates and concentrations for a slot angle of 25 degrees and a slot width equal to 2.54 mm.

where the injection flowrate was equal to 400 ml/min for an injection concentration of 400 ppm. This comparison demonstrates the reproduceability of the data.

In addition to the drag reduction data, measurements of additive concentration in the near-wall region at various points downstream of the injection slot were made during the injection process for several combinations of the independent variables. Figure 11 shows a typical plot of near-wall concentration, as a function of distance downstream of the injection slots. As before the distance is normalized with the no-injection channel shear velocity and the kinematic viscosity of the channel water. Peak values of concentration for various experimental conditions are presented in Table 3; a more comprehensive compilation of concentration data is contained in Appendix B.

Of interest here is the magnitude of the drag reduction achieved for the levels of concentration measured from x^+ = 30,000 to 70,000. Drag reduction levels are on the order of 20% for concentrations less than 1 ppm. The measured concentrations (0.6 ppm) are typical of the fully mixed concentration for this injection flowrate and injection concentration. These results demonstrate the effectiveness of the additive once it has attained a drag reducing conformation even if the additive concentration is at a very low level.

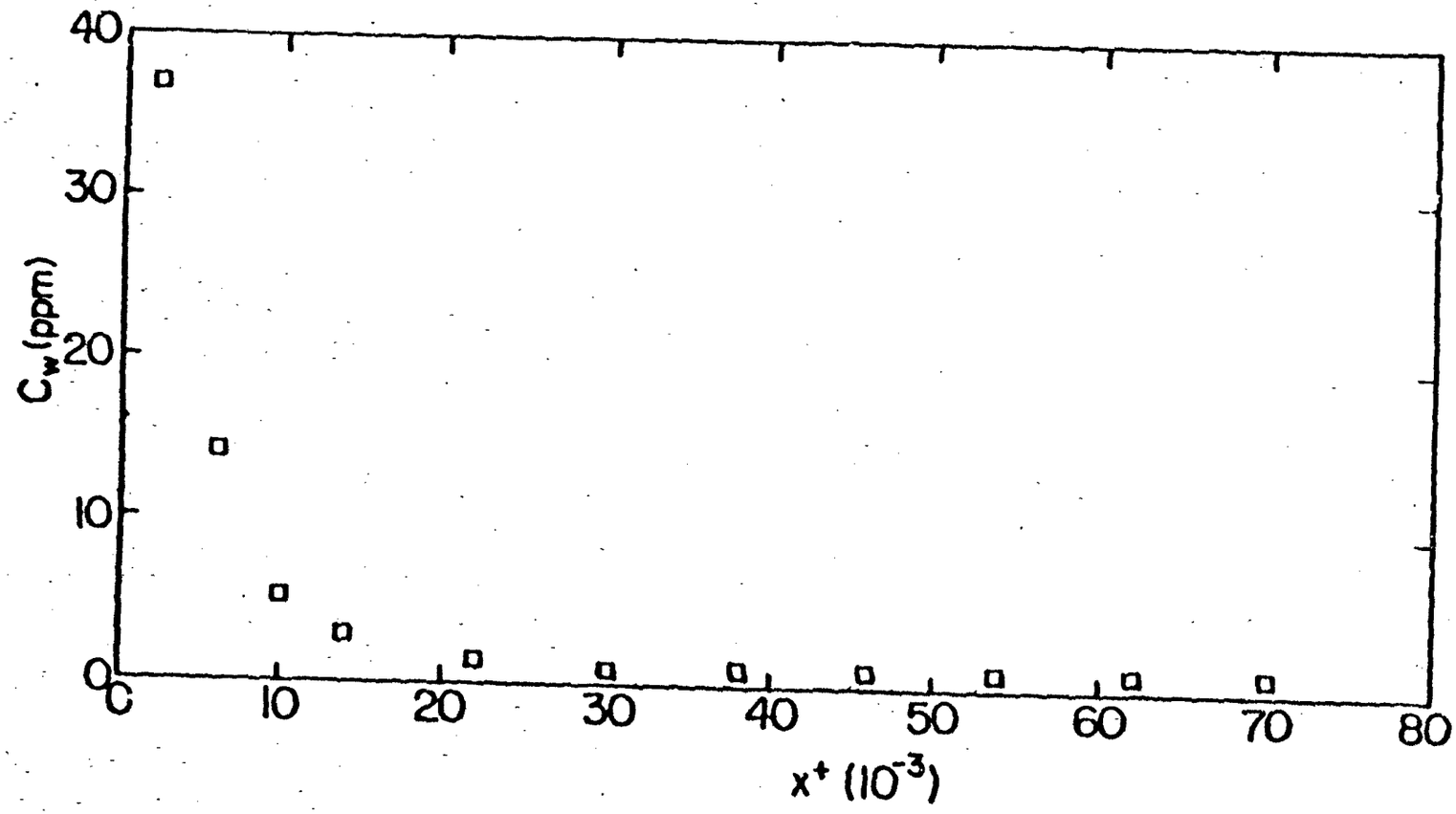

Figure 11. Variation of near-wall concentraiton (C_w) with distance downstream of injection slot for injection flowrates, concentration slot angle and slot width equal to 400 ml/min, 400 ppm, 25 degrees and 2.54 mm respectively.

Table 3. Peak concentrations

Injection Flowrate (ml/min)	Injection Concentration (ppm)	Concentration (ppm)
Slot angle=25°	Slot width=2.54 mm	
400	400	9.1
200	400	2.9
Slot angle=15°	Slot width=2.54 mm	
400	400	20.0
400	100	24.35
200	400	10.5
200	100	10.3
Slot angle=15°	Slot width=1.27 mm	
400	400	14.0
400	100	4.9
200	400	5.1
200	100	3.3

REGRESSION ANALYSIS

Optimization of the additive injection process was conducted using the techniques of response surface methodology based upon factorial experimentation. To implement these methods, experiments were performed over a small, but significant, range of the independent variables and the response (the quantity to be maximized) was measured. These results were then used to fit a mathematical model of the response over this range using a suitable regression technique. Once the mathematical model was determined, the importance of a given independent variable in determining the response was evaluated statistically. Also, the direction of movement in the space of the independent variables which will produce the largest increase in the response was determined. The latter result is of prime importance in the optimization process.

Since the purpose of this study is to maximize the drag-reducing performance of the additive injection process, a suitable measure of the merit of a given experimental configuration was devised. This measure, termed the merit function, was defined as the area under the drag reduction curve from the point where positive drag reduction begins (x_o) to the point where the injection process ceases to be effective. This definition is equivalent to the product of the average drag-reduction and the dimensionless streamwise length over which the slot injection is effective.

With the injection of an additive into an external boundary layer, once the additive diffuses from the near-wall region it is dispersed into the free-stream and lost as a drag reducer. In a channel flow the additive is contained and continually mixes back into the near-wall region until eventually, there is only a very dilute homogeneous mixture of the additive. Once this homogeneous condition is reached, any drag reduction that occurs is due only to the presence of the additive and is not a function of how the additive was delivered to the flow. The point where this homogeneous region begins marks where the diffusion away from the near-wall region is completed. Since only the effect of the injection process is of interest, the integration for the merit function stops where the flow becomes homogeneous. Examination of wall concentration and drag reduction data indicates that this point is in the vicinity of $x^+ = 30{,}000$ for the conditions examined in this study. In practice the numerical values of the merit function defined above are quite large because the unit for non-dimensionalizing the length is small. Consequently the function (y) used in this report was multiplied by 10^{-3}. Thus the merit function is

$$y = 10^{-3} \int_{x_o}^{30{,}000} (XDR)dx^+$$

Merit functions were calculated for all of the experiments and the results were statistically analyzed using the techniques of response surface methodology. As discussed by Hunter (16),

the first step in the analysis is to define a set of normalized coordinate with the origin located in the center of the range of interest of the independent variables. These coordinates are defined as:

$$x_1 = (\text{slot angle} - 20^\circ)/5^\circ$$
$$x_2 = (\text{slot width} - 1.88\ \text{mm})/0.63\ \text{mm}$$
$$x_3 = (\text{injection flowrate} - 300\ \text{ml/min})/100\ \text{ml/min}$$
$$x_4 = (\text{injection concentration} - 250\text{ppm})/150\ \text{ppm}$$

The above definitions are chosen so that the levels of the independent variables investigated become plus and minus one for all of the independent variables. The levels and combinations of variables tested in terms of these new variables are presented in Table 4 along with the corresponding experimental merit function (y) for each combination.

Since only two levels of each independent variables were tested, the model chosen is linear with first order interactions.

$$y = b_o + b_1x_1 + b_2x_2 + b_3x_3 + b_4x_4 + b_{12}x_1x_2 + b_{13}x_1x_3 + b_{14}x_1x_4 + b_{23}x_2x_3 + b_{24}x_2x_4 + b_{34}x_3x_4$$

The last six terms of this model represent interactions between these independent variables. Each coefficient represents the relative portion of the total variance in the response that can be attributed to a given independent variable. A variable is significant only if the variance due to that variable is greater than that due to random error. It should be noted that since all

the experiments were not replicated, there is no way to separate random error from failure of the model to fit the data. Therefore all variance away from the fitted model is treated as random error.

Table 4. Experimental and modelled values of merit function for factorial design

x_1	x_2	x_3	x_4	y	y_m	y_L
1	1	1	1	820	821	827
1	1	1	-1	525	560	499
1	1	-1	1	714	735	674
1	1	-1	-1	308	339	345
1	-1	1	1	761	766	827
1	-1	1	-1	498	505	499
1	-1	-1	1	672	680	674
1	-1	-1	-1	345	284	345
-1	1	1	1	745	766	827
-1	1	1	-1	507	505	499
-1	1	-1	1	713	680	674
-1	1	-1	-1	226	284	345
-1	-1	1	1	848	821	827
-1	-1	1	-1	599	560	499
-1	-1	-1	1	730	735	674
-1	-1	-1	-1	367	339	345

When this model was fit to the experimental data using a least squares regression and the statistical significance of the estimated coefficients was tested, the only coefficients which, to 95% confidence, are significantly different from zero were b_3, b_4, b_{12} and b_{34}. The coefficients b_{12} and b_{34} are significantly different from zero but play only a minor part in predicting the response; the bulk of the variation in the response is accounted for by the coefficients b_3 and b_4. The final form of the model is:

$$y_H = 586.13 + 76.75x_3 + 164.25x_4 + 27.75x_1x_2 - 33.63x_3x_4$$

Examination of this model in terms of the definitions of the variables reveals that in this range of the independent variables, the response is dominated by the effects of injection flowrate and concentration. The fourth and fifth terms in the model show that there is to some extent an interaction of slot angle and slot width, and injection flowrate and concentration but statistically these are of secondary importance to the main effects due to concentration and flowrate.

For the levels of the independent variables tested in this study, the response predicted by this model (y_H) is also presented in Table 4 along with predictions calculated using just the linear portion of the model.

$$y_L = 586.13 + 76.75x_3 + 164.25x_4$$

It can be seen that the prediction of the five-term model is in very good agreement with the experimental results. The results predicted by the three-term linear model show that this model accounts for the bulk of the variance in the response. This result of the regression analysis confirms the conclusions based upon inspection of the drag reduction plots in Figures 3 through 6.

In addition to identifying the relative importance of the independent variables to the merit function, the regression

analysis provides valuable information for the optimization process. If the exact mathematical nature of the response is known, one way to reach an optimum response would be to choose a starting point and at that point calculate the gradient of the response with respect to the independent variables. This directional derivative gives the direction in the domain of the independent variables which yields the greatest increase in the response. The response is then calculated at intervals along the path prescribed by the gradient until a peak is reached. Once this peak occurs, the gradient is recalculated and the search takes a new direction. This sequence would be repeated until a maximum is reached.

This procedure also can be followed in an experimental optimization. An evaluation of the response function is replaced by an experiment and an evaluation of the gradient is replaced by the sequence of factorial experiments described previously. The regression analysis is the key step in evaluating this gradient. It provides a mathematical expression approximating the local variation of the response.

For this study, the estimated gradient of the response (merit function) when evaluated at the origin of the centered coordinates yields a result which is independent of slot geometry. Figure 12 shows the direction of steepest ascent in the x_3x_4 plane along with the estimated local variation in the response as predicted by the linear model ($\hat{y}_L$). It is along this line of steepest ascent ($x_3=0.47x_4$) that future experiments

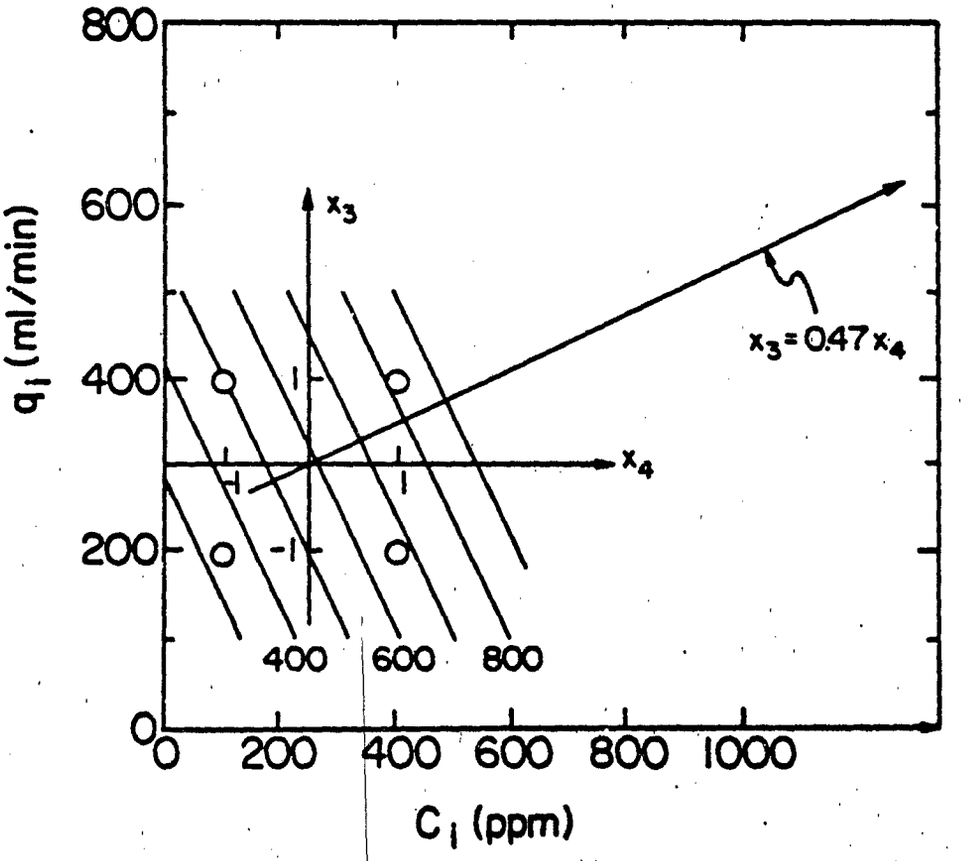

Figure 12. Superposition of dimensional and non-dimensional flowrate-concentration (q_1-C_1) planes showing estiamted contours of merit function and direction of steepest ascent.

should be conducted in order to approach an optimum most efficiently.

CONCLUSIONS AND RECOMMENDATIONS

The results of this study indicated that for the range of slot geometries, injection flowrates and additive concentrations examined, the performance, depends primarily upon the linear terms of injection concentration and injection flow rate. The product of injection concentration and flow rate as well as the product of slot angle and slot width were significant but less important. The statistical treatment of the results also yielded an estimate of the local gradient which in turn provides the direction in the domain of the independent variables to move in order to realize the largest increase in the merit function. The direction indicated involves increases in injection flowrate and additive concentration from the current levels. The increase in nondimensional flowrate (x_3) should be approximately one half the increase in nondimensional concentration (x_4).

Since the path for future experimentation indicated by this study will involve increases in injection flowrate, hence injection momentum flux, the question of whether the injection process is inherently independent of injector geometry, or was rendered so by a constraint imposed on normal momentum flux from the injector, will be answered during the course of further experimentation.

It is also important to note that additive concentrations less than 1 ppm yielded drag reduction of 20%. It is hypothesized that this occurred in these experiments because the

additives had attained an excellent conformation for drag reduction by the time they reached the locations where this result occurred.

REFERENCES

1. Tiederman, W.G. and D.G. Bogard. Wall Layer Structure and Drag Reduction - Role of viscous sublayer. Report No. PME-FM-81-2, Purdue University, W. Lafayette, Indiana, December 1981.

2. Tiederman, W.G. and T.S. Luchik. Wall Layer Structure and Drag Reduction - Bursting rates. Report No. PME-FM-82-2, Purdue University, W. Lafayette, Indiana, December 1982.

3. McComb, W.D. and L.H. Rabie. Local Drag Reduction Due to Injection of Polymer Solutions into Turbulent Flow in a Pipe. AIChE Journal, 28, 1982, pp. 547-565.

4. Maus, J.R. and L.R. Wilhelm. Effect of Polymer Injection on Frictional Drag in Turbulent Pipe Flow. J. Hydronautics, 4, 1970, pp. 35-39.

5. Walters, R.R. and C.S. Wells. An Experimental Study of Turbulent Diffusion of Drag-Reducing Polymer Additives. J. Hydronautics, 5, 1971, pp 65-72.

6. Fruman, D.H. and P. Galivel. Near-Field Viscoelastic Effects during Thin-Slit Drag-Reducing Polymer Ejection. J. of Rheology, 24, 1980, pp. 627-646.

7. Fruman, D.H. and P. Galivel. Anomalous Effects Associated with Drag-Reducing Polymer Ejection into Pure-Water Turbulent Boundary Layers. Viscous Flow Drag Reduction, Vol. 72, Progress in Astronautics and Aeronautics, ed. by G.R. Hough, AIAA, 1980, pp. 332-350.

8. Wu, J. and M.P. Tulin. Drag Reduction by Ejecting Additive Solutions into Pure-Water Boundary Layer. J. of Basic Engineering, 74, 1972, pp. 749-756.

9. Wu, J. Injection of Drag-Reducing Polymers into a Turbulent Boundary Layer. J. Hydronautics, 7, 1973, pp. 129-132.

10. Tullis, J.P. and K.L.V. Ramu. Drag Reduction in Developing Pipe Flow with Polymer Injection. BHRA International Conference on Drag Reduction, Sept., 1974, Paper G3.

11. Ramu, K.L.V. and J.P. Tullis. Drag Reduction and Velocity Distribution in Developing Pipe Flow. J. Hydronautics, 10, 1976, pp. 55-61.

12. Fruman, D.H. and M.P. Tulin. Diffusion of a Tangential Drag-Reducing Polymer Injection on a Flat Plate at High Reynolds Numbers. J. of Ship Research, 20, 1976, pp. 171-180.

13. Latto, B. and O.K.F. El Riedy. Diffusion of Polymer Additives in a Developing Turbulent Boundary Layer. J. Hydronautics, 10, 1976, pp. 135-139.

14. Wu, J., D.H. Fruman and M.P. Tulin. Drag Reduction by Polymer Diffusion at High Reynolds Numbers. J. Hydronautics, 12, 1978, pp. 134-136.

15. Reitzer, H., C. Oebel and M. Bues. Diffusion of macromolecular solutions in the turbulent boundary layer of a cylindrical pipe-Evolution of wall concentration. Rheologica Acta, 20, 1981, pp. 35-43.

16. Hunter, J.S. Some Applications of Statistics to Experimentation. Chem. Eng. Prog Symp. Series, AIChE, 56, No. 31, pp. 10-26.

Appendix A - Concentration Sampling Technique

Concentration measurements were made as part of this study in order to establish a data base for future investigation of the diffusion characteristics of these additives. Since it has been shown recently in our laboratory (1,2) and independently verified (3) that these additives have a direct effect on the structure of the buffer region of the flow, the additive concentration in this region is the quantity of interest.

All concentration measurements were made using samples of fluid drawn from the near-wall region through taps located flush with the surface of the channel wall. The taps were 1.6 mm in diameter and the samples were collected at a rate of 20 ml/min over a time period of one to one and one half minutes. This sampling rate is the lowest practical rate which can be maintained using the present facilities.

The rationale for using this sampling rate (Q_s), and not a higher one is demonstrated in Figure A-1, which compares measured concentrations for two sampling rates. It can be seen from this plot that when the sampling rate is increased from 20 ml/min to 40 ml/min there is a marked decrease in measured concentration in the region $4{,}000 < x^+ < 10000$. If peak drag reduction, which occurs in this region, is equivalent to a peak in buffer region concentration then this decrease in measured concentration would indicate that the fluid sampled at 40 ml/min included fluid from outside the buffer region, hence outside the area of interest.

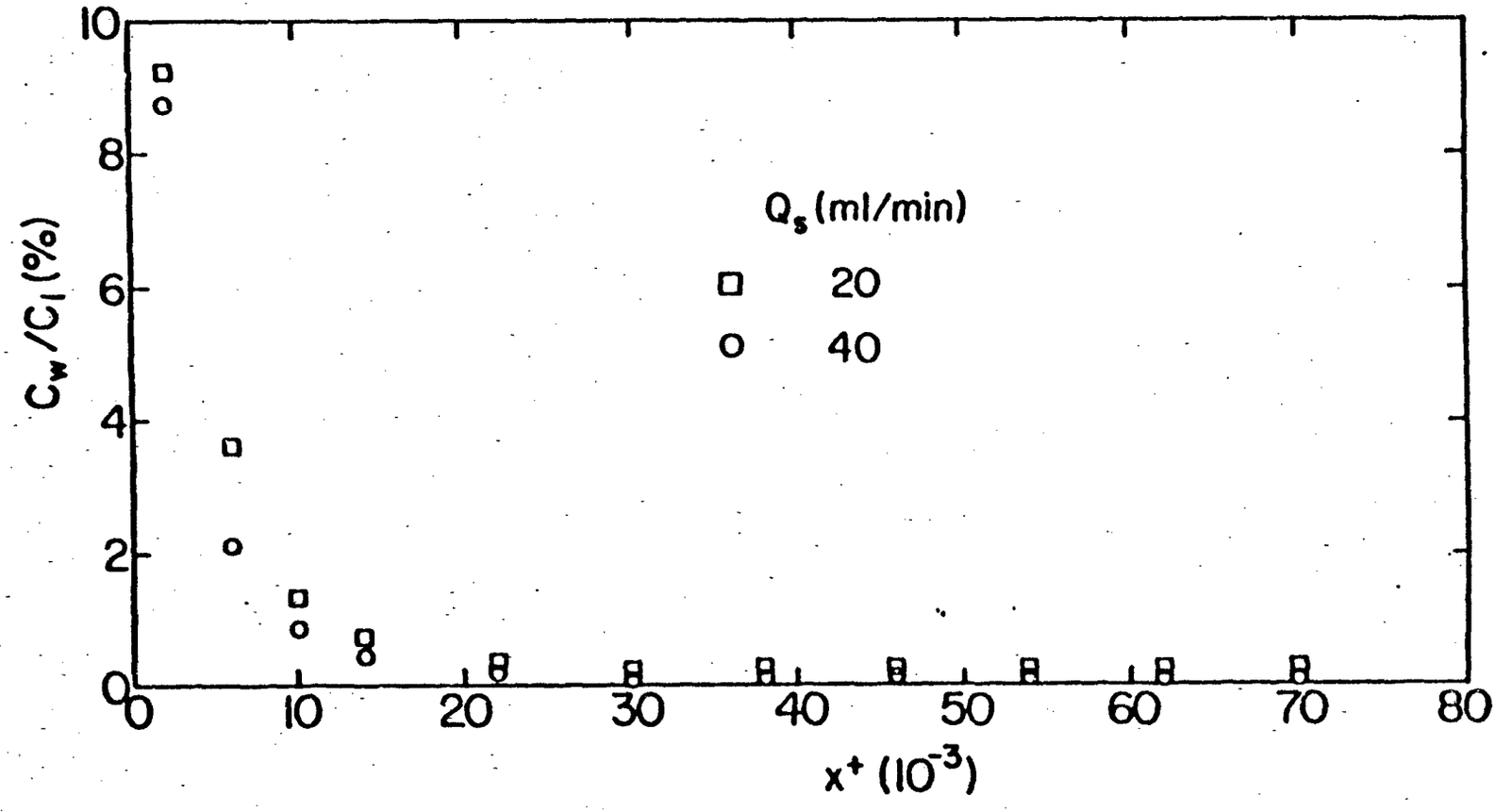

Figure A-1. Variation of near-wall concentration (C_w) as percent of injected concentration (C_i) downstream of injection slot for various sampling rates (Q_s).

Thus, the lower of the two flowrates was chosen.

Appendix B - Concentration Results

slot angle: 25 degrees
slot width: 2.54 mm
injection flowrate: 200 ml/min
injection concentration: 400 ppm

$x^+ \times 10^{-3}$	concentration (ppm)
2.00	11.60
10.00	0.68
22.00	0.56
54.00	0.36

slot angle: 25 degrees
slot width: 2.54 mm
injection flowrate: 400 ml/min
injection concentration: 400 ppm

$x^+ \times 10^{-3}$	concentration (ppm)
2.00	36.47
6.00	14.90
10.00	5.42
14.00	3.32
22.00	1.13
30.00	.59
38.00	.59
46.00	.54
54.00	.49
62.00	.49
70.00	.49

slot angle: 15 degrees
slot width: 1.27 mm
injection flowrate: 200 ml/min
injection concentration: 400 ppm

$x^+ \times 10^{-3}$	concentration (ppm)
2.00	20.84
10.00	1.84
22.00	.64
34.00	.32

slot angle: 15 degrees
slot width: 1.27 mm
injection flowrate 400 ml/min
injection concentration: 400 ppm

$x^+ \times 10^{-3}$	concentration (ppm)
2.00	56.32
10.00	5.44
22.00	1.24
34.00	0.64

slot angle: 15 degrees
slot width: 1.27 mm
injection flowrate: 200 ml/min
injection concentration: 100 ppm

$x^+ \times 10^{-3}$	concentration (ppm)
2.00	3.31
10.00	.23
22.00	.06
34.00	.07

slot angle: 15 degrees
slot width: 1.27 mm
injection flowrate: 400 ml/min
injection concentration: 100 ppm

$x^+ \times 10^{-3}$	concentration (ppm)
2.00	5.01
10.00	.58
22.00	.21
54.00	.11

slot angle: 15 degrees
slot width: 2.54 mm
injection flowrate: 200 ml/min
injection concentration: 400 ppm

$x^+ \times 10^{-3}$	concentration (ppm)
2.00	42.48
10.00	2.28
22.00	.64
54.00	.48

slot angle: 15 degrees
slot width: 2.54 mm
injection flowrate: 400 ml/min
injection concentration: 400 ppm

$x^+ \times 10^{-3}$	concentration (ppm)
2.00	79.92
10.00	5.80
22.00	1.36
54.00	.72

slot angle: 15 degrees
slot width: 2.54 mm
injection flowrate: 200 ml/min
injection concentration: 100 ppm

$x^+ \times 10^{-3}$	concentration (ppm)
2.00	10.25
10.00	.69
22.00	.10
54.00	.04

slot angle: 15 degrees
slot width: 2.54 mm
injection flowrate: 400 ml/min
injection concentration: 100 ppm

$x^+ \times 10^{-3}$	concentration (ppm)
2.00	24.35
10.00	1.87
22.00	1.00
54.00	.26

Appendix C - List of Publications and Presentaton

The following list summarizes the publications and presentations during the period 01 March 1983 to 29 February 1984.

1. Luchik, T.S. and W.G. Tiederman. Bursting Rates in Channel Flows and Drag-Reducing Channel Flows. Presented at the Symposium on Turbulence, University of Missouri-Rolla, September 26, 1983.

Appendix D - Distribution List

Dr. Michael M. Reischman, Code 432
Office of Naval Research
Arlington, VA 22217

Office of Naval Research Resident Representative
The Ohio State University Research Center
1314 Kinnear Road
Columbus, Ohio 43212

Director, Naval Research Laboratory
ATTN: Code 2627
Washington, DC 20375 (6 copies)

Defense Technical Information Center
Bldg. 5, Cameron Station
Alexandria, Virginia 22314 (12 copies)

Mechanical Engineering Business Office
Purdue University
W. Lafayette, IN 47907

James H. Green, Code 634
Naval Ocean Systems Center
San Diego, CA 92152

Dr. R.J. Hansen, Code 5844
Naval Research Laboratory
Washington, DC 20375

Dr. D.L. Hunston
Polymer Sciences & Standards Division
National Bureau of Standards
Washington, DC 20234

Mr. G.W. Jones
Code 5543
Naval Sea Systems Command
Washington, DC 20362

Dr. G.C. Lauchly
ARL
Pennsylvania State University
P.O. Box 30
State College, PA 16801

G. Leal
Department of Chemistry & Chemical Engineering
California Institute of Technology
Pasadena, CA 91125

Justin H. McCarthy
Code 1940
David Taylor Naval Ship R&D Center
Bethesda, MD 20084

Professor E.W. Merrill
Department of Chemical Engineering
Massachusetts Institute of Technology
Cambridge, MA 02139

Dr. T.E. Pierce
Code 63R31
Naval Sea Systems Command
Washington, DC 2:362

Professor W.W. Willmarth
Department of Aerospace Engineering
University of Michigan
Ann Arbor, MI 48109